Transactions of the **14th International Conference on Structural Mechanics in Reactor Technology** (SMiRT 14), Lyon, France, August 17-22, 1997 **L06/3**

Mechanical properties of 316L(N) stainless steel for intermediate strain rates at 20° and 550° C

Sainte Catherine C.(1), Yuritzinn T.(1), Sirvent A.(1), Cariou Y.(2), Martelet B.(3)
(1) CEA, France
(2) Framatome, France
(3) EDF, France

Abstract

Safety analysis for fast breeder reactors require that the energy which could be released in the primary system during a severe accident must be contained. Mechanical consequences of the accident must be therefore evaluated by taking into account the effect of dynamic loading. In order to produce a correct correlation between the finite element code computations and the real behaviour, an accurate determination of the material constitutive laws is required.

Introduction

For fast breader reactors, when considering the case of severe accidents, the safety analysis must show that the consequence can be confined inside the containment. This capability is based on the absorption, by deformation without fracture of the main vessel, of the impulsive released energy by the core disruptive accident and by the subsequent impact of sodium and of the broken inner structures.
One must therefore evaluate the mechanical behaviour of reactor structures by taking into account the effect of dynamic loading. In order to be able to perform realistic finite element computations, a determination of the material constitutive laws for different strain rates is required.
So, to determine such an equation which relates the flow stress to the applied strain and strain rate, we used a servo-hydraulic machine for $\dot{\varepsilon} = 10^{-3}$ and 7 s^{-1}, and an impact charpy testing device for $\dot{\varepsilon} = 150\ s^{-1}$.

Material, Test Domain and Specimen Type

Material

The austenitic stainless steel used is a special batch of 316L with low nitrogen contents. It has been produced by "Creusot Loire Industrie (CLI)" and the corresponding chemical composition is given in table 1. It is delivered as 20 mm thick plates and is heat treated by rapid cooling from 1100°C to 20°C by water.

C	Mn	Si	P	S	Cr	Ni	Mo	Co	N	B	Cu
0.026	1.8	0.18	0.022	0.012	17.6	12.1	2.5	0.23	0.07	0.0006	0.24

Table 1 : *Chemical composition of 316 L(N) stainless steel(weight percent).*

Test domain

The solicitation rate is generally quantified in terms of strain rate $\dot{\varepsilon}$ corresponding to $d\varepsilon/dt$. It is useful to keep in mind some order of magnitudes. One can by this way distinguish four rate domains (figure 1) :

- By quasi-static tests, we intend test for which $\dot{\varepsilon} < 10^{-2}$ s^{-1}. This rate range is generally covered by conventional electro-mechanical machines.
- An intermediate rate domain starts from 10^{-2} up to 10 s^{-1}. It corresponds to a range which is accessible with conventional servo-hydraulic machines.
- A domain corresponding to dynamic tests ranging from 10 up to 1000 s^{-1} is very badly covered by classical testing machines. Only the instrumented Charpy machine, generally used for impact testing, can give some rates around 100 s^{-1}. Otherwise, specific machines are required (high speed rotating machine, pneumatic machine, servo-hydraulic machine with accumulator...).
- The range of very high rates over 10^3 s^{-1}, is relevant from shock testing technics (Hopkinson bars, guns...).

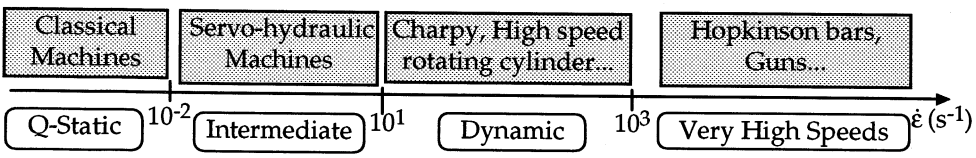

Figure 1 : *Deformation rate scale and associated references.*

Specimens types and sampling

The tensile specimens have all been taken with their axis perpendicular to the rolling direction. Two types of specimens have been used for these tensile tests :

- Two sections cylindrical tensile specimens with 5 and 8 mm (figure 2-a) ;
- Classical cylindrical tensile specimens with 5 mm diameter (figure 2-b).

These two types of specimens can be used with the servo-hydraulic or the instrumented Charpy machine. But, the specimen with two sections is designed to be instrumented by a gauge on the biggest section. This section remains elastic during the test, so the gauge signal can be used for the measurement of the stress during the test via the Young modulus. It is particularly useful in the case of instrumented Charpy machine because the original gauges are on the hammer and are only used for Charpy impact tests. As the tensile specimen is installed on the back part of the hammer, the normal gauges do not detect any signal.

This type of specimen with two sections comes from the ESIS draft entitled "Proposed Standard Method for Dynamic Tensile Tests" ([1]). In this document, different specimens shapes are proposed. The one selected here has been designed by MPA Stuttgart and finite element analysis reinforce this choice ([2]).

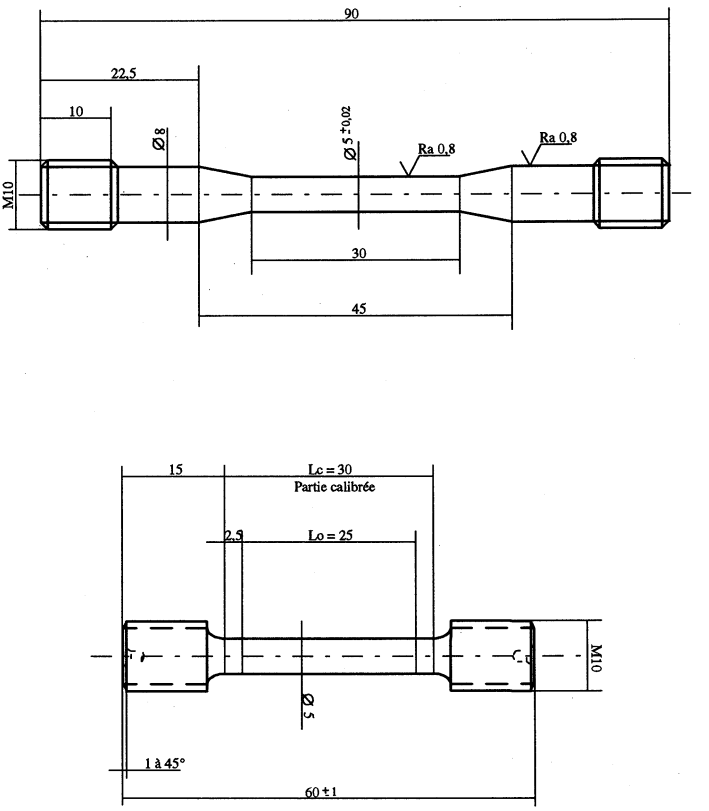

Figure 2 : *Tensile specimens schemes.*

Tensile performed tests at 10^{-2} and 7 s^{-1} on servo-hydraulic machine

Test machine and instrumentation

Quasi-static and intermediate rate tests were performed with a conventional servo-hydraulic machine (Instron 1273 of 10 tons capacity with 8500+ electronic command). The furnace is a lamp system working in air environment up to 900°C.

The tests performed combine two temperatures and two solicitation rates. The jack velocity corresponding to $\dot{\varepsilon}$ of 0.001 and 5 s^{-1} are respectively equal to 1.8 mm/min and 9.10^3 mm/min (0.15 m/s). This last speed is the maximum possible with the servo-hydraulic machine Instron 1273.

For all the tests, we stored the load, the jack displacement, the time and the temperature. Furthermore, for tests at $\dot{\varepsilon}$ =0.001 s^{-1}, we also stored the deformation of the homogeneous smooth part of the tensile specimen with an extensometer in order

to get a better precision. For, the tests performed on tensile specimens with two sections, we will add a gauge (EA-09-125AD-120 type) on the big section in order to compare it with the machine load cell.

Tests results

The main results of these tests are presented in the following table :

Test Ref.	T (°C)	$\dot{\varepsilon}$ (s^{-1})	E (GPa)	σ_y (MPa)	σ_m (MPa)	Ag (%)	A (%)	Z (%)
ADC-T1	20	10^{-3}	222	287	628	56	69.3	83.3
ADC-T2	20	6.8	-	415	662	43	59.3	76.5
ADC-T3	550	10^{-3}	138	140	439	35	43.4	76.1
ADC-T4	550	10^{-3}	142	138	441	35	43.5	73.7
ADC-T5	550	7	-	192	406	32	43.4	81.4
ADC-T6	550	7	-	187	410	31	39.7	79.3
ADC-D1	20	10^{-3}	-	273	602	58	72.9	82.6
ADC-D2	20	3.3	-	370	632	44	59.1	76.1

Table 1 : *Characteristic values issued from tensile tests on the servo-hydraulic machine. σ_y is the yield strength, σ_m is the ultimate tensile strength, Ag is the deformation at the maximum, A is the deformation at fracture and Z is the striction.*

The engineering curves are presented on a common graph on the following figure. We can observe the effect of temperature and also the effect of strain rate. The temperature increase gives a high softening degree. On the other side, the strain rate gives a clear hardening at 20°C but almost no effect at 550°C except on the deformation at fracture.

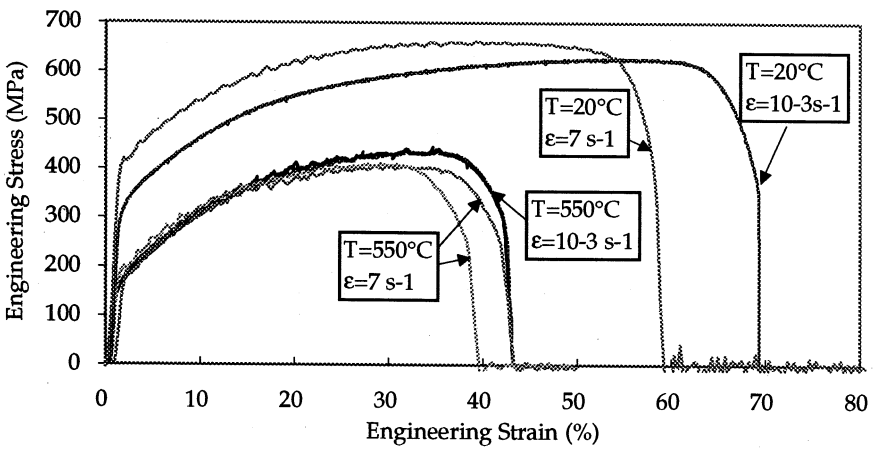

Figure 3 : *Engineering tensile curves at 20°C and 550°C for two solicitation rates.*

But, the solicitation rate does not remain constant during all the test. This is due to the length increase of the specimen during the test. The next figure shows an example of the evolution of the strain rate during the test. This evolution is linearly decreasing because the jack velocity remains constant during the specimen length increase. It is the initial rate which is indicated in table 1.

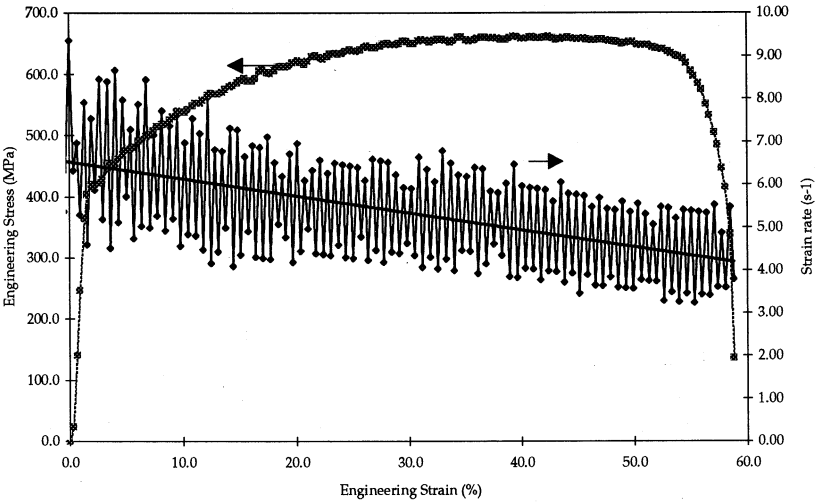

Figure 4 : *Tensile curve for ADC-T2 specimen and corresponding variation of strain rate.*

Comparison of load cell and gauge signals

The tensile specimens ADC-D1 and D2 had two sections. So, gauges have been paste on the biggest section and the corresponding signal has been recorded. From this signal, the knowledge of the Young modulus and a section correction, we can obtain a measurement of the stress in the specimen. This measurement has been compared to the signal coming from the load cell of the servo-hydraulic machine. The next figure compares the two engineering curves that we can construct from these signals for ADC-D2 specimen ($\dot{\varepsilon}$ =3.3 s^{-1}).

The agreement between the two curves is quite good. There is only a little over-estimation of the ultimate tensile strength σ_m (681 MPa rather than 632 MPa ≅ 8%).

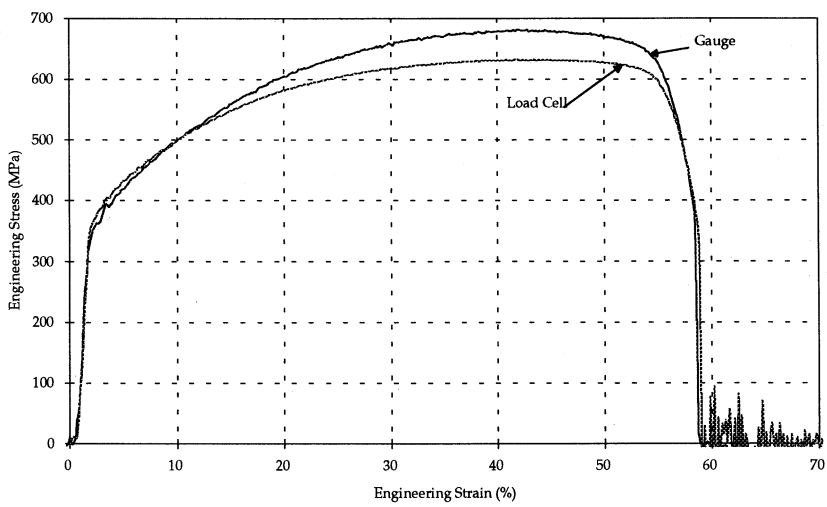

Figure 5 : *Engineering curves (ADC-D2) constructed from gauge signal or from load cell.*

Tests with Instrumented Charpy

Instrumented Charpy machine can achieve tensile tests with solicitation rates around 150 s^{-1}. This rate cannot be achieved with classical hydraulic machines. The general scheme of this test device is presented on figure 6. The tensile specimen is fixed on the back of the hammer and a ring is fixed at the other end of the specimen in such a way that it cannot go throw the supports when the hammer will be at the vertical.

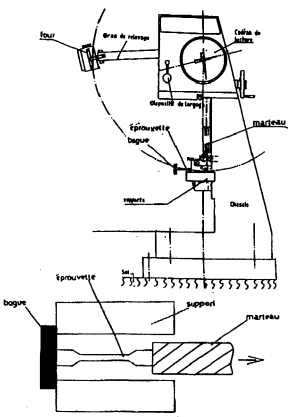

Figure 6 : *Instrumented Charpy testing machine.*

A sheathe furnace is used for the tests at 550°C. It is attached to the lifting arm of the hammer and stay with this one. When the hammer is delivered, the tensile specimen go out of the furnace sheathe and is slightly cooled (-6°C) during its fall before the impact. The temperature is stored during this operation and the relevant temperature is the temperature at impact. In all the cases, the displacement during the impact is recorded (optical sensor) as a function of time and also the derivative of this signal giving the rate. For the test at room temperature, we used a gauge (EA-09-125AD-120) stick on the 8 mm diameter part in order to measure the stress. For the tests at 550°C, we cannot use gauge on the specimen, so we used a little load cell located between the tensile specimen and the hammer. All the signals were stored on a Kontron 1 MHz oscilloscope.

Test results on instrumented Charpy machine

At room temperature (20°C), the energy required in order to break tensile specimens is around 190 Joules. Figure 7 gives an example of engineering curve obtained with an impact energy of 300 Joules.

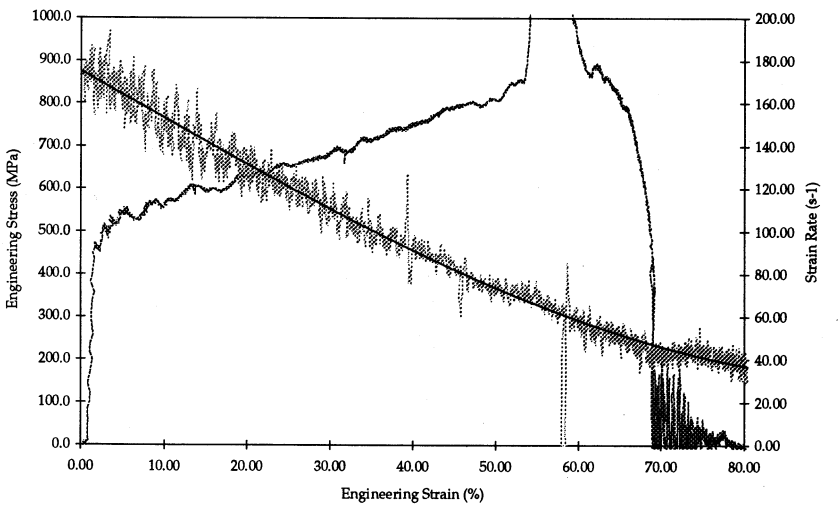

Figure 7 : *Engineering tensile curve at 20°C obtained on the impact Charpy machine with an initial energy of 300 Joules and associated strain rate curve (specimen ADC-D4).*

The strain rate is far from being constant during this type of test. The maximum rate is obtained during the elastic deformation. Then, it decreases regularly in the plastic range. This is due not only to the specimen elongation, but also to the slowing down of the hammer due to the energy absorption for the deformation of the specimen.
We can also notice the abrupt saturation of the gauge signal just before the specimen broke. This saturation has not been suppressed even with different precautions concerning the axially and the slacks.

Discussion and Comparison with Results coming from Literature

In order to represent the influence of strain rate, it is interesting to draw the yield stress versus in a half-logarithm graph. Figure 8 shows our results with some results coming from the literature.
Our results are in very good agreement with those coming from the literature. The corresponding adjusted equations are as follow :

At 20°C : $$\sigma_y(\text{MPa}) = 15.6 \cdot \text{Ln}(\dot{\varepsilon}) + 385 \quad (1)$$

At 550°C : $$\sigma_y(\text{MPa}) \cong 150 \text{ MPa} \quad (2)$$

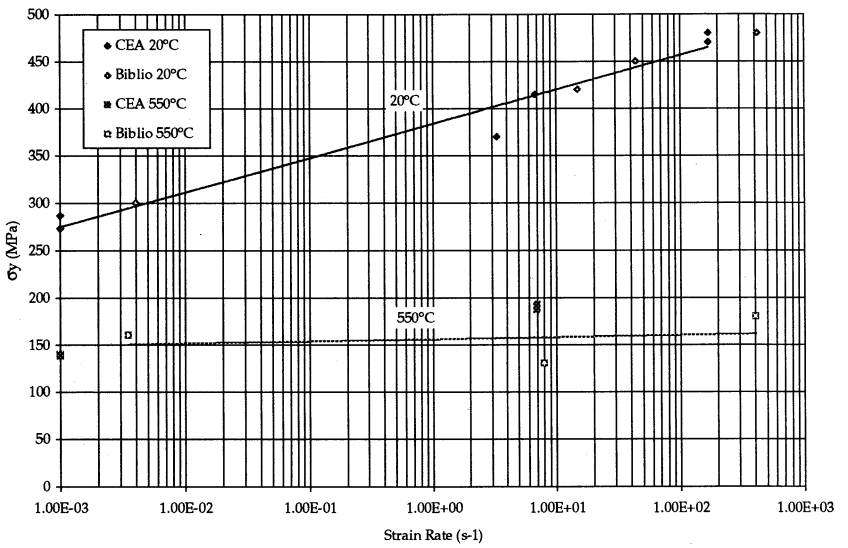

Figure 8 : *Yield stress versus strain rate at 20°C and 550°C and comparison with [3].*

The ultimate tensile strength (σ_m) at 20°C increases in the same order. But, the value at 170 s^{-1} obtained with the instrumented Charpy is clearly greater than the value obtained at intermediate strain rate. In fact, its value (880 MPa) seems disproportional in front of those obtained at intermediate strain rate (650 MPa). This can be explained by the fact that this value is very near the perturbation above mentioned on this signal. The value measured at 550°C seems to remain constant as for yield strength. On the other hand, the elongation and striction at fracture decrease when the strain rate increase.

In terms of material law, the true stress/true strain curves obtained at different strain rates for room temperature is presented on figure 8. This dependence can be fitted by the empirical Symonds and Cowper law :

$$\sigma_d = \sigma_s \cdot \left(1 + \left(\frac{\dot{\varepsilon}}{D}\right)^{1/p}\right) \quad (3)$$

In our case, the corresponding parameters are D = 1914 MPa and p = 3.00 even if the fitting for the high strain rate is relatively poor for strain larger than 5%.

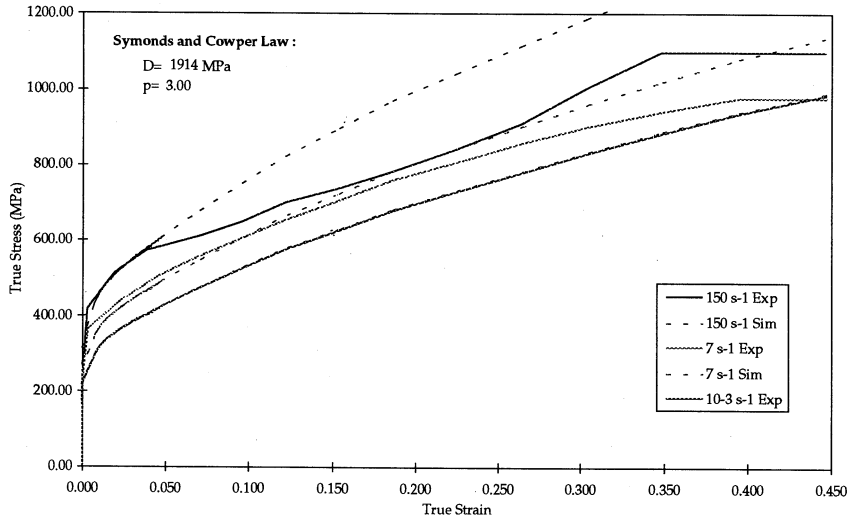

Figure 9 : *True stress/true strain curves at 20°C for the different strain rates.*

Conclusions

These tensile tests give us the austenitic stainless steel (316 L(N)) material laws for different temperatures (20 et 550°C) and strain rates ranging from 0.01 up to 150 s^{-1}. They also give us the opportunity to precisely define the tests conditions and the instrumentation, in particular for the instrumented Charpy testing machine with tensile specimens.

As mentioned in the literature, our results show a logarithmic dependence of yield stress and mechanical strength with strain rate at room temperature. But at 550°C, the influence of strain rate is negligible. The dependence with strain rate of elongation and striction at fracture is decreasing. We got the complete loading curves and the true-stress/true-strain curves. A Symonds-Cowper law is then fitted to these experimental curves in order to use it as a material constitutive equation taking into account the strain rate in finite element codes.

References

[1] ESIS, *"Proposed Standard Method for Dynamic Tensile Tests"*, TC 5, Draft 3, October 1994.

[2] YURITZINN T., *"ADC - Simulation Numérique de l'Essai de Traction Dynamique"*, CEA Saclay, Rapport DMT/95-638, (1995).

[3] ALBERTINI C., DEL GRANDE A. and MONTAGNANI M., *"Effects of Irradiation on the Mechanical Properties of Austenitic Stainless Steels under Dynamic Loading"*, in Effects of Radiation on Structural Materials, ASTM STP 683, (1979), pp. 546-556.

[4] SAINTE CATHERINE, *"ADC - Effets de la Température et de la Vitesse de Déformation sur les Propriétés Mécaniques des Aciers Inox"*, CEA Saclay, Rapport DMT/95-465, (1995).

[5] MARSCHALL C.W., LANDOW M.P. and WILKOWSKI G.M., *IPIRG Program"*, NUREG/CR-6098, BMI-2175, Battelle Report, OH, USA, October, (1993).